UDC 303.732.4, 519.816
DOI: 10.20535/SRIT.2308-8893.2022.2.08

AUTOMATIC PANCREAS SEGMENTATION USING RESNET-18 DEEP LEARNING APPROACH

S.N. KAKARWAL, P.M. PAITHANE

Abstract. The accurate pancreas segmentation process is essential in the early detection of pancreatic cancer. The pancreas is situated in the abdominal cavity of the human body. The abdominal cavity contains the pancreas, liver, spleen, kidney, and adrenal glands. Sharp and smooth detection of the pancreas from this abdominal cavity is a challenging and tedious job in medical image investigation. Top-down approaches like Novel Modified K-means Fuzzy clustering algorithm (NMKFCM), Scale Invariant Feature Transform (SIFT), Kernel Density Estimator (KDE) algorithms were applied for pancreas segmentation in the early days. Recently, Bottom-up method has become popular for pancreas segmentation in medical image analysis and cancer diagnosis. LevelSet algorithm is used to detect the pancreas from the abdominal cavity. The deep learning, bottom-up approach performance is better than another. Deep Residual Network (ResNet-18) deep learning, bottom-up approach is used to detect accurate and sharp pancreas from CT scan medical images. 18 layers are used in the architecture of ResNet-18. The automatic pancreas and kidney segmentation is accurately extracted from CT scan images. The proposed method is applied to the medical CT scan images dataset of 82 patients. 699 images and 150 images with different angles are used for training and testing purposes, respectively. ResNet-18 attains a dice similarity index value up to 98.29±0.63, Jaccard Index value up to 96.63±01.25, Bfscore value up to 84.65±03.96. The validation accuracy of the proposed method is 97.01%, and the loss rate value achieves up to 0.0010. The class imbalance problem is solved by class weight and data augmentation.

Keywords*:* Deep Learning, Dice Coefficient, Fully Connected Layer (FCN), Residual Network (ResNet-18), Visual Geometry Group (VGG).

INTRODUCTION

Image splitting task is rigorously act as vital character in image investigation [1]. Image splitting task is beneficial for many applications like clinical image analysis, disease detection of crop, traffic control observation, metallic surface crack detection, and Aerospace image analysis. CT, MRI, PET, and supplementary images are used in the clinical image diagnosis and cure of illnesses. Pancreas segmentation is challenging job in medical image investigation and analysis [2]. Accurate organ segmentation and rapid processing are the major challenges in the result of medical images. Computerized segmentation of several image subsections is useful to analyze anatomical organization as well as abdominal body. Segmentation is played major role in visualization and diagnosis of clinical images. Sub-grouping is an important subject to several image-processing research. Spleen, liver, kidney, pancreas is present in the abdominal CT images [3]. Bottom-up approach and Top-down approach are applied to image splitting process [4]. In Top-down approach, medical image segmentation is performed within minimum time- period but less accuracy of segmentation. Bottom-up approach is

efficient approach for medical image segmentation with high accuracy and minimum time-period. Semantic segmentation is one approach of deep learning which used for abdominal computed tomography. Deep learning model is popular approach of a machine learning methods. Deep learning model is dealing with algorithms with hierarchical procedure layers [5]. It is experimenting nonuniform transformations to view and gain data characteristics successfully [6]. Currently Deep learning model is popular in various domains such as medical image analysis, medical signal analysis, speech recognition, bio informatics, computer vision [4]. Convolution neural networks, Generative Adversarial Networks, networks with auto-encoder, and recurrent neural networks are prominent deep learning approaches. These approaches are introduced and used in various task to map with state-of-the-art results. In deep learning, network training is required with dataset. For network training, set of convolution network, annotated dataset, optimizer, minibatch size, epoch, loss function is used. Dataset can be divided into training, validation and testing purposed also. Fully convolution network (FCN) was introduced by Long et al. [5]. In FCN, fully convolution layer is used as the last fully convolution network layer. For more accuracy of dense pixelwise predication, the network is used fully convolution network. Semantic segmentation can be performed by FCN. FCN architecture is built with pooling, upsampling and convolution. FCN can perform predication of image within on single forward pass [7].

MATERIALS AND METHODS

Image Dataset and Ground Truth Labeling

Bottom-UP approaches are applying on a dataset of 80 patient, 53 male and 57 female patients high resolution (512*512) CT scan images of 3D abdominal with 1,5–2,5 mm slice thickness range using Philips and Siemens MDCT scanners [2]. The 63 patients CT scans abdominal images are erratic recommend by an expert radiologist from the Picture Archiving and Communications System (PACS). National Institutes of Health Clinical Center is providing database of CT dicom images for abdominal,78 to 79 years patient age series with a mean of 46.8±16.7 are used dataset [8]. DICOM medical images are converted to PNG image format. The view of scans images was axial, sagittal and coronoal with 1,5 mm or 3 mm thickness available [9]. Human expert labeling was performed under guideline of certified radiologist. 3 labels are created for manual labeling like background, pancreas, and kidney. Medical images are selected with different focal phase angle of CT. Size and shape of pancreas is varies in different view of CT. Image input size is $255 \times 255 \times 3$,699 images are used for and 150 for testing.

LevelSets Algorithm

Levelset algorithm was presented by Osher and Sethian. It can use zero corresponding exterior method [10]. Basic phenomena are to adjustment of portable pathway of a two-dimensional arc into portable path of a 3D surface. In this, level Set is actively participate toward indication of arcs as zero levelset of high dimension hyper-superficial [9]. Challenge of such exercise suggestions supplementary faultless algebraic execution also operates topological variation without any prob-

lems [8]. The predictable set edge is described zero levelset of an implicit symbol U of the evolving curve. In brief, evolve the implicit levelset function $\phi(x,y,t)$ to represent evolution of curve $\tau(t)$ with a speed $F(x,y)$ in normal direction. Time *t*, zero levelset $(x, y)/\ \phi(x,y,t)=0$ defines evolved shape $\tau(t)$:

$$\phi(\tau(t),t)=0\,. \tag{1}$$

Differentiate equation (1) with respect to *t* and apply chain rule,

$$\frac{\partial\phi}{\partial t}+\nabla\phi.\frac{\partial\tau}{\partial t}, \tag{2}$$

F denotes speed of curve in normal direction, describe below

$$\frac{\partial\tau}{\partial t}.N=F\,, \tag{3}$$

where *N* denotes outwards normal, and elaborated by equation

$$N=\frac{\nabla\phi}{|\nabla\phi|}\,. \tag{4}$$

Substitute Equation (4) and (3) into (2), and calculate evolution equation for ϕ as

$$\phi_t+F|\nabla\phi|=0\,.$$

This is fundamental equation of the levelset [6], and zero levelset represents item shape curve:

$$\tau(t)=\{(x,y)/\phi(x,y,t)=0\}\,.$$

Function ϕ is generally determined grounded on signed distance calculation to primary front. Relating to image field purely based on Euclidean distance between the curve and one image point. Describe below:

$$\phi(x,y)=\pm d(x,y)\,,$$

where $d(x,y)$ — Euclidean distance from point to borderline. Sign: points inside borderline (–) sign and outside (+) sign.

Evolution of borderline is elaborated by partial differential equation on zero levelset of ϕ:

$$\frac{\partial\phi}{\partial t}=-F|\nabla\phi|\,,$$

where F — known function, which calculated by the local curvature κ at the zero levelset, i.e., $F=F(\kappa)$, where κ:

$$\kappa=\nabla.\frac{\nabla\phi}{|\nabla\phi|}=\frac{\phi_{xx}\phi_y^2-2\phi_x\phi_y\phi_{xy}+\phi_{xy}\phi^2}{(\phi_x^2+\phi_y^2)^{3/2}}\,.$$

Speed function F is represent as $F=F(L,G,I)$, where L — local information, which define by local geometric properties, G — global property of front depends on contour and location of front; I — independent properties that independent of front [11].

The propagating task is characterized as:

$$\frac{\partial \phi}{\partial t} = g_I (F_A + F_G) |\nabla \phi| .$$

The term *FA*, causing front to consistently multiply or bond with a speed of *FA* dependent on sign [12].

FG : portion that relate on geometry of front, such as own local curvature:

$$g_I (x, y) = \frac{1}{1 + \left|\nabla (G_\sigma \otimes I(x, y))\right|},$$

where $G_\sigma \otimes I$ — convolute image *I* with Gaussian smoothing filter G_σ with characteristic width of σ.

The form of speed function expressed as [9]: $F = FA + FG$. Via calculation control objects or different image force which stated in common but simple form:

$$F = A(F_A + F_G) + B ;$$

$$A = \frac{1}{(1 + dist(C_{img}, C_{front})} ;$$

$$B = \overrightarrow{dist}(C_{img}, C_{front}) .$$

dist() — appropriate distance function which is used to calculate variance of image features between propagating front and propagated zones. *B* — additional forces from image content. *C* — image content model, including any of the color, shape, and texture features.

Automatic Seeded Region Growing Algorithms for LevelSet

General area developing algorithms determine pixel value physically from each mark region as seed. The seed point normally contains of great uniform to neighboring pixels and can be correspond to region [9]. The nature of seed point is very close together to cluster center in clustering algorithm. AP clustering algorithm is going to discover seed points in an image [13].

All data points as potential cluster centers, and computes accessibility and accountability data by equations below iteratively between every two data points to find characteristic centers of data points:

$$R(i,k) \leftarrow S(i,k) - \max_{k' \partial t, k' \neq k} \{a(i,k') + S(i,k)\} ,$$

if $$i \neq k, ai,\ k \leftarrow \min\left\{0, R(k,k') + \sum_{i' \partial t . i' \notin i,k} \max\{0, ri', k\}\right\},$$

$$a(k,k) \leftarrow \sum_{i' \partial t . i' \neq k} (0, R(i',k)) .$$

To receive the seed x_j by equation below and cluster this holds x_i :

$$\underset{1 \le j \le N}{\operatorname{argmax}} [R(i,k) + a(i,k)] .$$

The simple linear iterative cluster (SLIC) algorithm is going for segmented pixel-level image before using AP clustering process by combining adjacent pixels with similar characteristics to some irregular pixel blocks [14].

The region growing is computed by continually assimilation of seed points also surrounding pixels and division of aim objects with background. Lastly design of ROIs is in rectangular boxes according to segmentation results [10].

Euclidean Distance runs to measure LAB color matches by equation

$$S = \sqrt{(L_0 - L_{0j})^2 + (a_0 - a_{0j})^2 + (b_0 - b_{oj})^2} \ .$$

PROPOSED METHOD

Residual Network (ResNet-18)

The training accuracy problem is solved by Residual Network-18 (ResNet-18). $H(x)$ is underlying mapping layer fit to new layer with x map inputs from previous layer. Residual function is stated that $f(x) = H(x) - x$ with same dimensions. So updated residual function $f(x) + x$ is use in deep network layer [15].

Residual function is used to improve training accuracy value with minimum time.

This residual function is used in every connected layer which formulated using following expression:

$$F = f(x, \{M_i\}) + x \ . \tag{5}$$

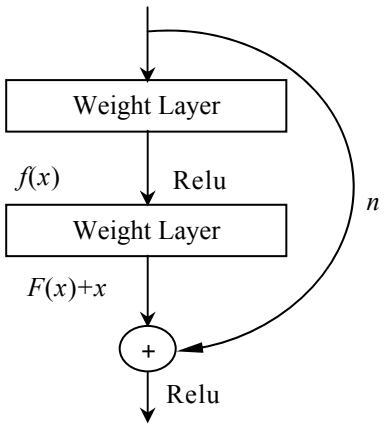

Fig. 1. ResNet-18 Relu Function

In this x and F are input and output dimensions, M_i is layer used for RELU. $F(x) + x$ is used as short connection in ResNet-18 (Fig. 1). Linear projection can be execute through M_s and add into eq. (5) when dimension will match. M_s is square matrix which address the training accuracy problem when matching dimensions condition satisfied [16]:

$$F_u = F + M_s x \ .$$

Table 1. ResNet-18 model Network Layer Detail

Layer Name	Output Size	ResNet-18 Layer
Conv1	112×112	7×7.64 Stride,2
Conv2	56×56	3×3 max pool, stride 2
		$\begin{bmatrix} 3\times3,64 \\ 3\times3,64 \end{bmatrix}\times 2$
Conv3	28×28	$\begin{bmatrix} 3\times3,128 \\ 3\times3,128 \end{bmatrix}\times 2$
Conv4	14×14	$\begin{bmatrix} 3\times3,256 \\ 3\times3,256 \end{bmatrix}\times 2$
Conv5	7×7	$\begin{bmatrix} 3\times3,512 \\ 3\times3,512 \end{bmatrix}\times 2$
	1×1	

Table 1 is depicted detail about convolution network layer used in ResNet-18 approach.

Data Augmentation

Class imbalance is problem in deep learning image segmentation. An image data augmenter setup to an examine of pre-processing choices for image augmentation, such as resizing, rotation and reflection. Random *x* and *y* direction translation is performed by [−10,10] and random rotation by [−180,180]. Data augmentation is beneficial to enhance output and results of deep learning approaches using set novel and discrete examples to datasets [17]. Transformations in datasets by using data augmentation approaches authorize companies to minimize these experimental costs. In the system, data augmentation is using reflection, translation, and rotation to improve model prediction accuracy and reducing overfitting of data [18].

Loss Function

Cross Entropy. Cross -Entropy is used in ResNet-18 as loss function to relate binary classification problems that calculate the probability of specific class or not [19]. Let d and g represent the input image and related ground truth or manually annotated image respectively. The key aim of segmentation is to learn relation of *d* and *g*. Cross-entropy loss function L_{CET} is shown as

$$L_{CET} = \sum_{i=1}^{N} g_i \log(f_i(d,t)) + (1-g_i)\log(1-f_i(d,t)),$$

where $i =$ pixel index, $N =$ total pixel.

Dice Loss. To calculate overlap rate of predicated mask and ground-truth for segmentation results Dice Score Coefficient is used. DSC is formulated as below:

$$DSC(d,g) = \frac{2(d \cap g)}{|d| + |g|}.$$

Dice loss function can be formulated as per below expression:

$$L_{DSCL} = \sum_{c}(1 - DSC_c),$$

where C is number of iteration.

Categorical Cross-Entropy Loss. It is used for multi-class classification task. In this work 3 class are used liked background, pancreas, and kidney. This model helps to detect object belong to which class among other classes.

Categorical loss function computed using following expression:

$$L_{CCET} = \frac{1}{N}\sum_{p}^{N} -\log\left(\frac{e^{s_p}}{\sum_{j}^{C} e^{s_j}}\right),$$

where M is positive class, e^{s_p} is score of positive class.

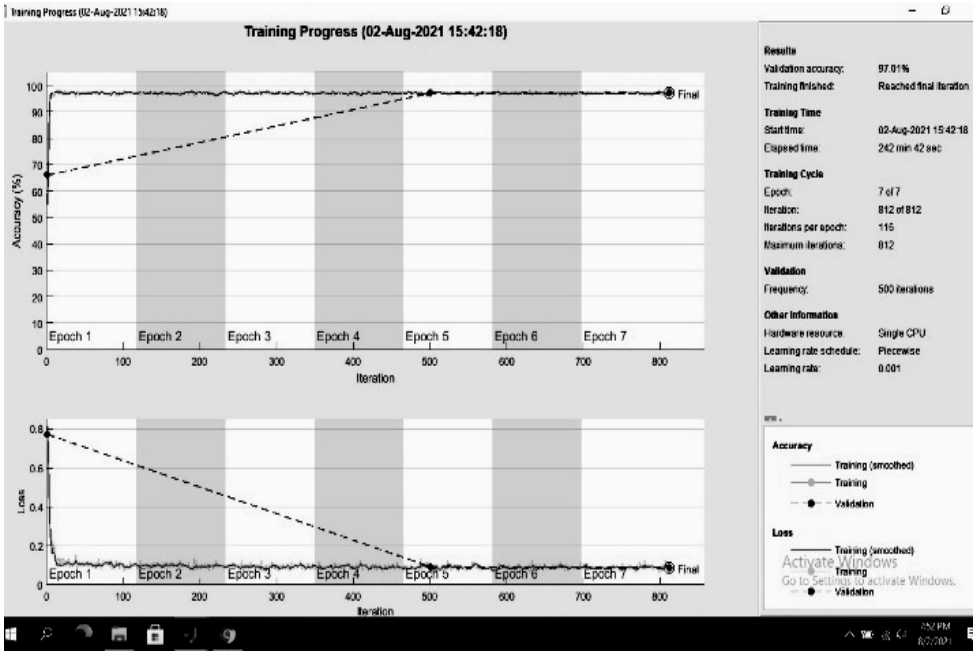

Fig. 2. ResNet-18 Validation Accuracy

RESULTS

Evaluation Parameter

Global Accuracy (*GA*): *GA* is the ratio of perfectly segmented pixels divided by the total number of pixels

$$GA = \frac{\sum_{i=0}^{C} p_i}{\sum_{i=0}^{C}\sum_{j=0}^{C} p_{ij}},$$

where p_{ij} is the number of pixels of class *i* segmented as belonging to class j.

Mean Accuracy (*MA*): Mean Accuracy is an next step of Global Accuracy, in which the ratio of match pixels are computed in a per-class pattern and then averaged over the total number of classes [19]:

$$MA = \frac{1}{C+1}\sum_{i=0}^{C}\frac{p_{ii}}{\sum_{j=0}^{C}p_{ij}}.$$

Interaction of Union (*IoU*): Jaccard index alias *IoU*, it is correlation between segmented image (S) and annotated image (B). The value of *IoU* lies between 0 to 1[20].

$$Jaccard(d,g) = \mathrm{IoU} = \frac{|d \cap g|}{|d \cup g|}.$$

Mean Interaction of Union (*MIoU*): Mean *IoU* is calculated by the average *IoU* value of all classes.

$$MIoU = \frac{\sum_{C} IoU}{C},$$

where total number of classes value is denoted by C. 3 classes are used like pancrea, kidney and background.

Weighted Interaction of Union:

$$WIoU = \frac{\sum_{C} IoU * \sum_{i=0}^{C} p_i}{C}.$$

Weight value is number pixel in class. Average *IoU* of each class [19].

Bfscore. The bf score measure how close to the segmented boundary of an input image matched with the annotated image. The BF score is calculated with the help of the harmonic mean of the precision and recall values with a distance error tolerance to decide whether a point on the segmented boundary has a correlated to annotated boundary or not [20]:

$$score = \frac{2 * precision * recall}{(recall + precision)}.$$

Dice Coefficient. It is correlation between segmented image (S) and annotated image (B). The value of dice coefficient lies between 0 to 1 and easily converted into % for understanding purpose [20]:

$$dice(S,B) = 2 * \frac{|S \cap B|}{(|S| + |B|)}.$$

Sensitivity

$$Sensitivity = \frac{TP}{FN + TP},$$

where *TP* is true positive, *FN* is false negative [20].

Specificity

$$Specificity = \frac{TN}{FP + TN},$$

where *TN* is true negative, *FP* is false positive [20].

Table 2. ResNet-18 Model Compare with VGG-16 and VGG-19

Approach	VA, %	Bf, %	Number of Layer	Time	MA, %
ResNet-18	97.01	84.06±3.96	18	242 min 42 sec	42.16
VGG-16	97.01	84.05±4.02	16	522 min 7 sec	42.439
VGG-19	96.90	56.62±2.48	19	632 min 44 sec	42.05

Table 2 is depicted performance of ResNet-18 as compared other deep learning approaches. Validation accuracy is more as compared to VGG-19. ResNet-18 is required less training time. The Bf score of ResNet-18 is higher as compared to VGG-16 and VGG-19. ResNet-18 is using 18 number of layer where 17 number are convolution layer used so accuracy is improved.

Table 3. ResNet-18 Model Compare with VGG-16 and VGG-19 using Evaluation Parameter

Approach	IOU	Dice	Sensitivity	Precision
ResNet-18	96.63 ± 01.25	98.29 ± 00.63	96.78 ± 00.03	96.64 ± 00.12
ATLAS [19]	55.50 ± 17.10	69.60 ± 16.70	67.90 ± 18.20	74.10 ± 17.10
U-net Single Mode [20]		74.10 ± 00.13	74.30 ± 00.17	78.90 ± 00.13
Frame-1[2]	57.2 ± 25.40	68.80 ± 25.60	72.50 ± 27.20	71.50 ± 30.00
Frame-2[2]	57.9 ± 13.60	70.70 ± 13.00	74.40 ± 15.10	71.60 ± 10.50
LevelSET[1]	28.18 ± 14.07	42.26 ± 16.37	98.48 ± 00.03	98.70 ± 00.03

Table 3 is depicted the performance of ResNet-18 deep learning approach as compared to state-of-arts. ResNet-18 having more IoU value as compared to other approach. In Dice index, ResNet-18 is achieved higher value (Fig. 3).

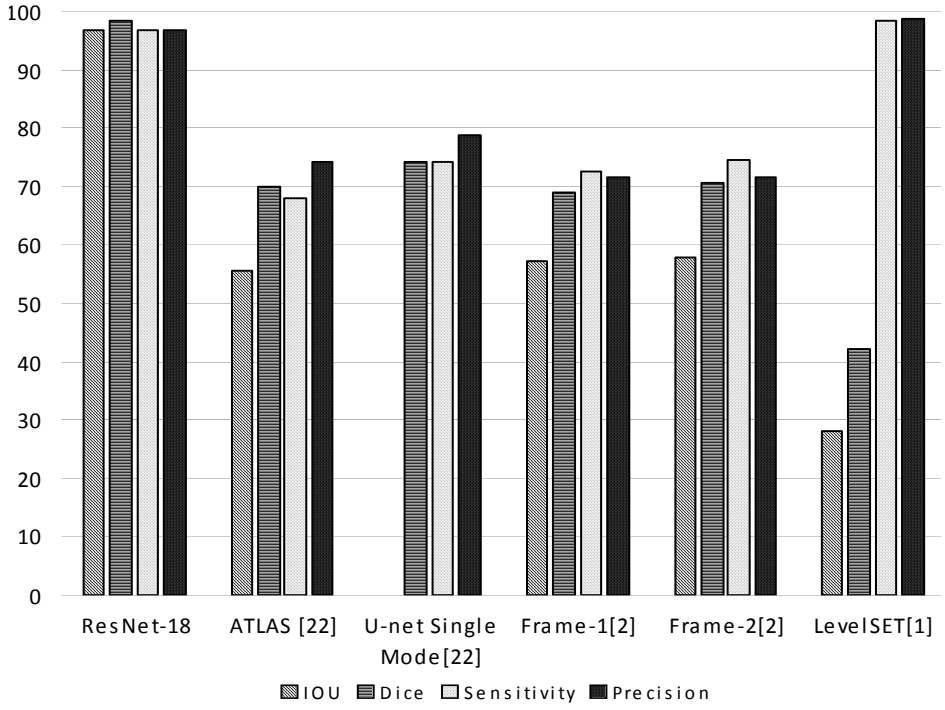

Fig. 3. ResNet-18 Result Comparison with State-of-Art

Above figure is showing the ResNet-18 result in detail in terms of IOU, Dice, Sensitivity and Precision (Fig. 4 and 5).

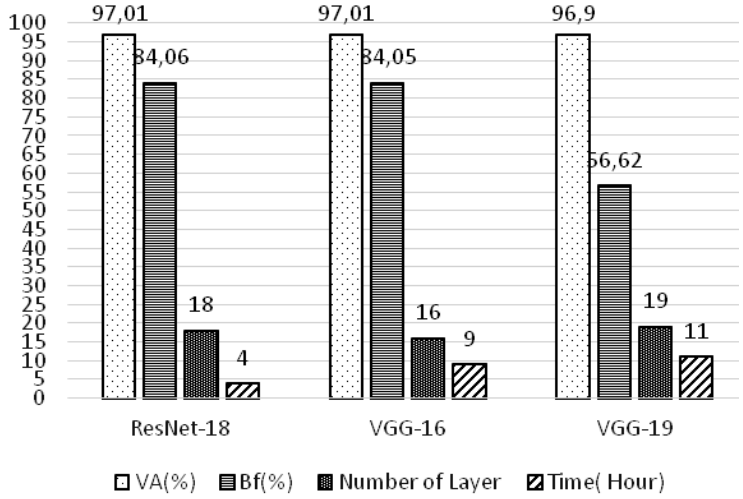

Fig. 4. ResNet-18 Result Comparison with State-of-Art using Performance Parameter

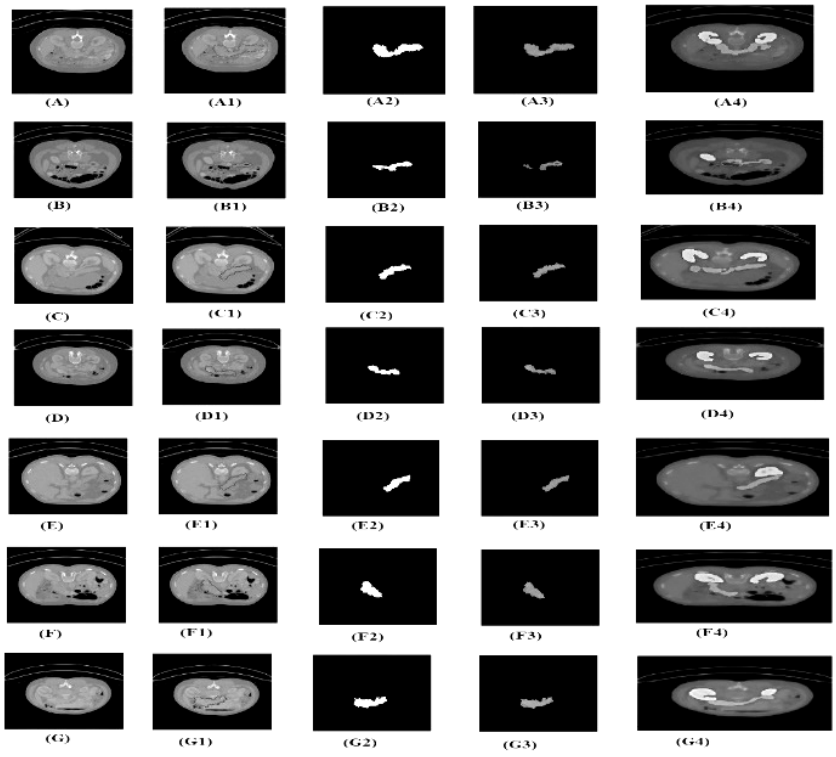

Fig. 5. ResNet-18 Result Comparison with State-of-Art using Performance

Above figure is consist of origan image (subfigure A, B, C, D, E, F, G), levelset boundary image (subfigure A1, B1, C1, D1, E1, F1, G1), binary levelset (subfigure A2, B2, C2, D2, E2, F2, G2), segmented image by levelset (subfigure A3, B3, C3, D3, E3, F3, G3) and Segmented image using ResNet-18 (subfigure A4, B4, C4, D4, E4, F4, G4).

CONCLUSION

ResNet-18 approach for automatic pancreas segmentation from CT scan images. 18 layers architecture is used for multiple organ segmentation from CT scan image. In VGG-16 method, 16 convolution layers are used, in VGG-19, 19 convolution layers are used. In deep learning, training of network layer is time consuming task. Levelset method is also used for pancreas segmentation but if seeded point is wrong then output image is not correct. Levelset algorithm takes more time to extract image with non-clear boundary of pancreas. Proposed method takes very less time as compared to other deep learning method. Bfscore value of proposed method is superior from VGG-19 method for same dataset. Sensitivity, Mean Accuracy and Mean-bfscore value are superior to other methods. Dice coefficient, jaccard Index are high as compared to state-of-art. Proposed method values as per evaluation matrix parameters are high as compared to state-of-art. Loss function value is less than other methods. In method, patch labeling is used so 64*64 patch channel used so only one organ segmentation can be performed. In proposed method, manually annotation process is performed by medical practitioner and two classes is generated for pancreas and kidney. With the help of proposed method many abdominal organ segmentations can be performed. Input image size is 255*255*3 used so maximum pixel information is available in convolution network. Noisy pixel image information can be easily omitted during dropout network layer. Accurate pancreas shape and size is detected by proposed method, but it fails to detect pancreas cancer affected areas in percentage. Pancreas size and shape is available in 2D image using proposed method. 3D pancreas image detection is future scope for proposed method.

AUTHOR CONTRIBUTIONS

Pradip Paithane: Conceptualization, Data curation, Methodology, Software, Roles/Writing-original draft. Dr.S.N. Kakarwal: Formal analysis, Investigation, Visualization, Project administration, Supervision, Validation, Writing - review and editing.

REFERENCES

1. Pradip M. Paithane, Dr.S.N.Kakarwal, and Dr.D.V.Kurmude, “Top-Down Method used for Pancreas Segmentation”, *International Journal of Innovative and Exploring Engineering (IJITEE)*, 9-3, pp. 2278–3075, 2020.
2. Amal Farag, Le Lu, Holger R. Roth, Jiamin Liu, Evrim Turkbey, and Ronald M. Summers, “A Bottom-Up Approach for Pancreas Segmentation Using Cascaded Superpixels and (Deep) Image Patch Labeling”, *IEEE Transactions on image processing*, 26-1, 2017. doi:10.1109/TIP.2016.2624198.
3. Pradip M. Paithane and S.A. Kinariwal, “Automatic Determination Number of Cluster for NMKFC-means algorithm on Image Segmentation”, *IOSR-JCE*, 17-1, 2015.
4. Pradip M. Paithane and Dr.S.N. Kakarwal, “Automatic Determination Number of Cluster for Multi Kenel NMKFCM algorithm on image segmentation”, *Intelligent System Design and Applications*, Springer Cham, 2017, pp. 80–89.
5. Justin Ker, Lipo Wang, Jai Rao, and Tchoyoson Lim, “Deep Learning Applications in Medical Image Analysis”, *IEEE Transactions*, pp. 9375–9389, 2018.

6. Yingege Qu, Pheng Ann Heng, and Tien-Tsin Wong, *Image Segmentation using the levelset Method*. New York: Springer, 2004.
7. Xin-Jiang, Renjie-Zhang, and Shengdong-Nie, "Image Segmentation Based on Level set Method", *International conference on Medical Physics and Biomedical Engineering*, Elsevier, 2012.
8. Joris R Rommelse, Hai-Xiang Lin, and Tony F. Chann, *A Robust Level Set Algorithm for Image Segmentation and its Parallel Implementation*. Springer, 2014.
9. P.M. Paithane, S.N. Kakarwal, and D.V. Kurmude, "Automatic Seeded Region Growing with Level Set Technique Used for Segmentation of Pancreas", *Proceedings of the 12th International Conference on Soft Computing and Pattern Recognition (SoCPaR 2020)*, 1383.
10. Qianwen Li, Zhihua Wei, and Cairong Zhao, "Optimized Automatic Seeded Region Growing Algorithm with Application to ROI Extraction", *IJIG*, 17-4, 2017.
11. H.K. Abbas, A.H. Al-Saleh, H.J. Mohamad, and A.A. Al-Zuky, "New algorithms to Enhanced Fused Images from Auto-Focus Images", *Baghdad Sci. J.*, 10, 18(1):0124, 2021
12. R.J. Mitlif and I.H. Hussein, "Ranking Function to Solve a Fuzzy Multiple Objective Function", *Baghdad Sci. J.*, 10, 18(1):0144, 2021.
13. O. Bandyopadhyay, B. Chanda, and B.B. Bhattacharya, "Automatic Segmentation of bones in X-ray images based on entropy measure", *Int. J. Image Graph.*, 16-01, 2016.
14. I. Bankman, *Handbook of medical imaging: processing and analysis*. New York: Acdameic Press, 2000.
15. Shuo Cheng and Guohui Zhou, "Facial Expression Recognition Method Based on Improved VGG Convolution Neural Network", *IJPRAI*, vol. 34, no. 7, 2020.
16. Pikul Vejjanugraha, Kazunori Kotani, Waree Kongprawechnon, Toshiaki Kondo, and Kanokvate Tungpimolrut, "Automatic Screening of Lung Diseases by 3D Active Contour Method for Inhomogeneous Motion Estimation in CT Image Pairs", *Walailak J. Sci.Tech*, 18-2, 2021
17. Mizuho Nishio, Shunjiro Noguchi, and Koji Fujimoto, "Automatic Pancreas Segmentation Using Coarse-Scaled 2D Model of Deep Learning: Usefulness of Data Augmentation and Deep U-Net", *Appl. Sci.*, 2020. doi: 10.3390/app10103360.
18. Srikanth Tammina, "Transfer Learning using VGG-16 with deep convolution Neural Network for classifying Images", *IJSR Publications*, 9-10, 2019.
19. H.R. Roth et al., *Deep Organ: Multi-level Deep Convolutional Networks for Automated Pancreas Segmentation*. MICCAI, 2015.
20. Robin Wolz, Chengwen Chu, Kazunari Misawa, Michitaka Fujiwara, Kensaku Mori, and Daniel Rueckert, Automated Abdominal Multi-Organ Segmentation With Subject-Specific Atlas Generation, *IEEE Transactions On Medical Imaging*, 32-9, 2013.

Received 04.01.2022

INFORMATION ON THE ARTICLE

S.N. Kakarwal, PES Engineering College, Aurangabad, MH, India.

Pradip M. Paithane, Dr. Babasaheb Ambedkar Marathwada University, Aurangabad, MH, India, e-mail: paithanepradip@gmail.com

АВТОМАТИЧНА СЕГМЕНТАЦІЯ ПІДШЛУНКОВОЇ ЗАЛОЗИ З ВИКОРИСТАННЯМ RESNET-18 МЕТОДУ ГЛИБОКОГО НАВЧАННЯ / С.Н. Какарвал, П.М. Паітане

Анотація. Точний процес сегментації підшлункової залози є важливим процесом для раннього виявлення раку підшлункової залози. Підшлункова залоза

розташована в черевній порожнині тіла людини як і печінка, селезінка, нирки та наднирники. Чітке та плавне виявлення підшлункової залози у черевній порожнині є складною та виснажливою роботою у ході дослідження медичного зображення. Для сегментації підшлункової залози в перші дні застосовуються підходи «зверху-вниз», як-от новий модифікований алгоритм кластеризації K-середніх (NMKFCM), масштабно інваріантне перетворення ознак (SIFT), алгоритм оцінювання щільності ядра (KDE). Останнім часом популярний метод BottomUp для сегментації підшлункової залози в аналізі медичного зображення та діагностики раку. Алгоритм LevelSet використовується для виокремлення підшлункової залози серед черевної порожнини. Поглиблене навчання, підхід «знизу-вгору» кращий, ніж інші. Глибока залишкова мережа (ResNet-18) глибоке навчання, підхід «знизу-вгору» використовується для виявлення точної та чіткої підшлункової залози за медичними зображеннями КТ. В архітектурі ResNet-18 застосовується 18 шарів. Автоматична сегментація підшлункової залози та нирок виокремлюється із зображень КТ-сканування із високою точністю. Запропонований метод застосовано на медичній комп'ютерній томографії 82 пацієнтів. 699 зображень і 150 зображень із різними кутами застосовують для навчання та тестування відповідно. ResNet-18 досягає значення індексу подібності кубиків до 98,29±0,63, значення індексу Жакара до — 96,63±01,25, значення Bfscore — до 84,65±03,96. Точність валідації запропонованого методу становить 97,01%, а значення коефіцієнта втрат досягає 0,0010. Проблема дисбалансу класу вирішується за допомогою ваги класу та збільшення даних.

Ключові слова: глибоке навчання, коефіцієнт кубиків, повністю підключений шар (FCN), залишкова мережа (ResNet-18), група візуальної геометрії (VGG).